International Journal of High Speed Electronics and Systems
Vol. 15, No. 3 (2005) 549–566

World Scientific
www.worldscientific.com

Equalizer Architectures for 40-Gb/s Optical Systems Limited by Polarization-Mode Dispersion

Jonathan Sewter
Anthony Chan Carusone[§]
Edward S. Rogers Sr. Department of Electrical and Computer Engineering
University of Toronto
10 King's College Rd.
Toronto, Canada, M5S 3G4
[§]*tcc@eecg.utoronto.ca*

An analysis of first-order polarization-mode dispersion (PMD) effects in a 40-Gb/s optical system is used to compare different electronic equalizer architectures as potential PMD compensators. Both linear and nonlinear equalizers are considered employing symbol-spaced and fractionally-spaced taps. It is found that a decision feedback equalizer consisting of a 3-tap symbol-spaced feedforward equalizer and a 1-tap feedback equalizer effectively eliminates PMD as the dominant length-limiting factor in most 40-Gb/s optical systems. Such an equalizer would entail less complexity than several previously reported electronic PMD compensators.

Keywords: optical communication, polarization mode dispersion, adaptive equalizer

1. Introduction

Optical communication systems have been used since the 1970s for high-volume data transmission within wide-area, metropolitan-area and local-area networks[1]. Until recently, long-haul links over single-mode fiber (SMF) could be designed without concern for the bandwidth limitations of the fiber. By compensating for fiber loss with amplifiers, the reach of these systems could be extended. To satiate the demand for greater network capacity, the data rate of current optical systems has been pushed to 10 and 40 Gb/s (OC-192 and OC-768). At these data rates, it is no longer possible to neglect the bandwidth limitations of SMF, as several dispersion mechanisms lead to frequency-dependent loss[2].

The two most important dispersion mechanisms for SMF are chromatic dispersion (CD) and polarization-mode dispersion (PMD). CD is a result of the wavelength-dependency of the refractive index of the fiber. PMD results from the variation in the refractive index of the fiber with respect to the polarization of the light signal. Since CD can be compensated by proper choice of optical fiber, PMD has been identified as the limiting factor in high-speed optical systems[3].

To mitigate the effects of PMD, optical systems must include some form of PMD compensation. This compensation can be achieved either optically or electronically.

Electronic PMD compensation schemes are attractive because they allow greater integration with existing circuitry, leading to more compact, less expensive solutions. This is especially true for wavelength-division multiplexed (WDM) systems, in which every channel needs PMD compensation[4]. Also, because PMD fluctuates with changes in temperature and environment, PMD compensators must be able to adapt to varying channel conditions within milliseconds[5]. Fast and accurate adaptation is more easily performed in the electronic domain. Successful electronic equalization has already been demonstrated at 10 Gb/s by Wu et al (7-tap FFE)[6], Bülow et al (8-tap FFE, 1-tap FBE)[7], and Möller et al (1-tap FBE)[8], and more recently at 40 Gb/s by Nakamura et al (3-tap FFE, 1-tap FBE)[9], and Hazneci and Voinigescu (7-tap FFE)[10].

While it has been shown that nonlinear equalization using a decision feedback equalizer (DFE) is required to reduce the power penalty caused by PMD to acceptable levels[11], the tradeoffs between different equalizer architectures are not evident. In this paper, a system-level analysis of PMD effects in a 40-Gb/s system using Matlab/Simulink is used to compare several equalizer architectures in terms of overall system performance, as has been done for optical compensation schemes[12]. Both linear and decision feedback equalizer (DFE) architectures are considered employing symbol-spaced and fractionally-spaced taps. Using this analysis we are able to quantify the increase in system reach that can be attained by equalization. Also, we show that effective compensation of PMD can be achieved using fewer taps in the feedforward equalizer (FFE) and feedback equalizer (FBE) than have been used in several previously reported implementations.

In Section 2 of this paper, the effects of PMD on optical transmission are reviewed and in Section 3 PMD compensation methods are broadly surveyed. Section 4 provides a description of the system model used for the Matlab/Simulink simulations. In Section 5 the various equalizer architectures considered for PMD compensation are described and Section 6 explains the methodology of the simulations performed. Finally, Section 7 contains the results of these simulations and Section 8 concludes the paper.

2. Polarization-Mode Dispersion (PMD)

PMD is a result of the phenomenon of birefringence which affects all real optical fibers. Birefringence refers to the difference in refractive index experienced by light in the two orthogonal polarization modes of the fiber. It is caused by ellipticity of the fiber cross-section due to asymmetric stresses applied to the fiber during or after manufacturing. Birefringence leads to fast and slow modes of propagation and consequently dispersion[13].

In terms of digital communications, PMD results to a first order in an input pulse being split into a fast and slow pulse which arrive at the receiver at different times, as shown in Figure 1. If the differential delay of the two pulses is significant compared to the bit period, intersymbol interference (ISI) and an increase in bit-

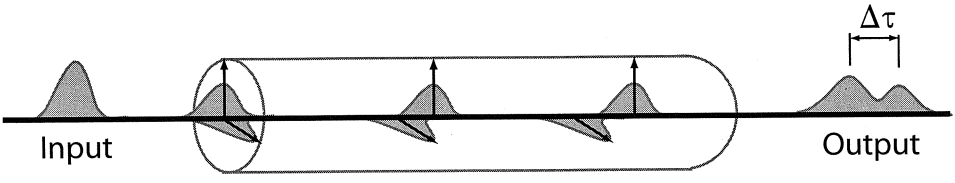

Fig. 1. Pulse bifurcation due to PMD. The power in the input pulse is split between the two polarization modes of the fiber. Birefringence causes a difference in phase velocities between the two modes, resulting in ISI at the output.

error rate (BER) will result.

2.1. *Consequences of PMD for Optical Systems*

To a first order, the impulse response of an optical fiber with PMD is[14]:

$$h_{\mathrm{PMD}}(t) = \gamma\delta(t) + (1-\gamma)\delta(t-\Delta\tau) \tag{1}$$

where γ is the proportion of the optical power in the "fast" state of polarization (SOP), (1-γ) is the proportion of power in the "slow" SOP and $\Delta\tau$ is the differential group delay (DGD) between the fast and slow components.

The parameters γ and $\Delta\tau$ vary depending on the particular fiber and its associated stresses; γ can take any value from zero to one with uniform probability throughout this range[15], and $\Delta\tau$ varies statistically according to a Maxwellian distribution[16] given by:

$$\rho(\Delta\tau) = \sqrt{\frac{2}{\pi}}\frac{\Delta\tau^2}{\sigma^3}e^{-\frac{\Delta\tau^2}{2\sigma^2}} \tag{2}$$

The constant σ in (2) is related to the average DGD, $\Delta\tau_{avg}$, by[17]:

$$\sigma = \frac{\sqrt{2\pi}\Delta\tau_{avg}}{4} \tag{3}$$

Therefore, though it can occasionally assume large values, $\Delta\tau$ will for the most part remain close to its average value. Furthermore, $\Delta\tau$ varies over time with significant variations sometimes observed on the order of milliseconds[5].

The average DGD per unit length of a fiber is defined as its PMD parameter, which has units of ps/$\sqrt{\mathrm{km}}$. Typical installed fibers exhibit a PMD of 0.5 - 2.0 ps/$\sqrt{\mathrm{km}}$[18]. New fibers can be manufactured with a PMD of as low as 0.05 ps/$\sqrt{\mathrm{km}}$[19]. Given the PMD parameter, the average DGD of a fiber of length L is given by:

$$\Delta\tau_{avg} = \mathrm{PMD} \times \sqrt{L} \tag{4}$$

It has been calculated that to prevent PMD from causing system outages amounting to more than thirty seconds per year (corresponding to an outage probability of 10^{-6}), the average DGD must be less than approximately 15% of a bit period, T_B[3].

$$\Delta\tau_{avg} < 0.15T_B \tag{5}$$

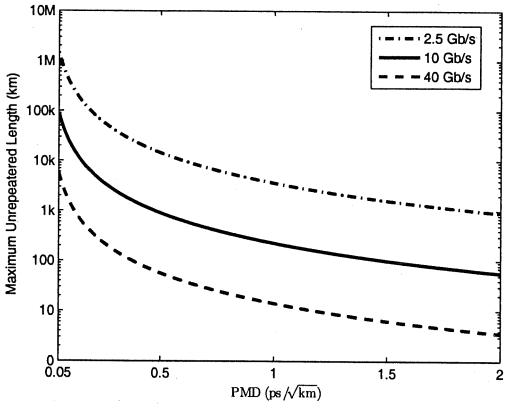

Fig. 2. Plot of maximum unrepeatered link length for fibers with varying PMD parameters for 2.5-, 10- and 40-Gb/s optical systems, assuming PMD is the dominant limiting factor.

This has severe implications as the data rate of these systems is increased to 10 and 40 Gb/s. As the data rate is increased on a given fiber, the maximum useful length of the fiber decreases according to the square of the increase. For example, given a fiber with a PMD of 1.0 ps/$\sqrt{\text{km}}$ and using (5), the maximum length of a 2.5-, 10- and 40-Gb/s system is 3600, 225 and 14 km, respectively, if PMD is the limiting factor. This relationship is illustrated in Figure 2.

2.2. *PMD Frequency-Domain Analysis*

The frequency-domain characteristic of an optical fiber with PMD can be easily obtained by taking the Fourier transform of its impulse response, $h_{\text{PMD}}(t)$, as defined in (1). The transfer function, $H_{\text{PMD}}(f)$, is described by:

$$H_{\text{PMD}}(f) = \gamma + (1-\gamma)e^{-j2\pi f \Delta\tau} \tag{6}$$

which is equal to:

$$H_{\text{PMD}}(f) = \gamma + (1-\gamma)[\cos(2\pi \frac{f}{f_{DGD}}) - j\sin(2\pi \frac{f}{f_{DGD}})] \tag{7}$$

where $f_{\text{DGD}} = \frac{1}{\Delta\tau}$. By inspection of (7), it can be seen that $|H_{\text{PMD}}(f)|$ has maximae at $f = kf_{\text{DGD}}, k \in I$, and minimae at $f = \frac{(2k-1)}{2} f_{\text{DGD}}, k \in I$.

Magnitude and phase plots of $H_{PMD}(f)$ for varying PMD conditions (γ and $\Delta\tau$) are shown in Figure 3.

From these plots it is apparent that the frequency response of a PMD fiber varies greatly depending on the specific nature of the PMD conditions. In general, PMD can cause notches in the frequency response of the fiber. The frequency of these notches is proportional to the DGD. The depth of these notches is dependent on γ, with the case $\gamma = 0.5$ resulting in nulls. The wide variation in potential frequency

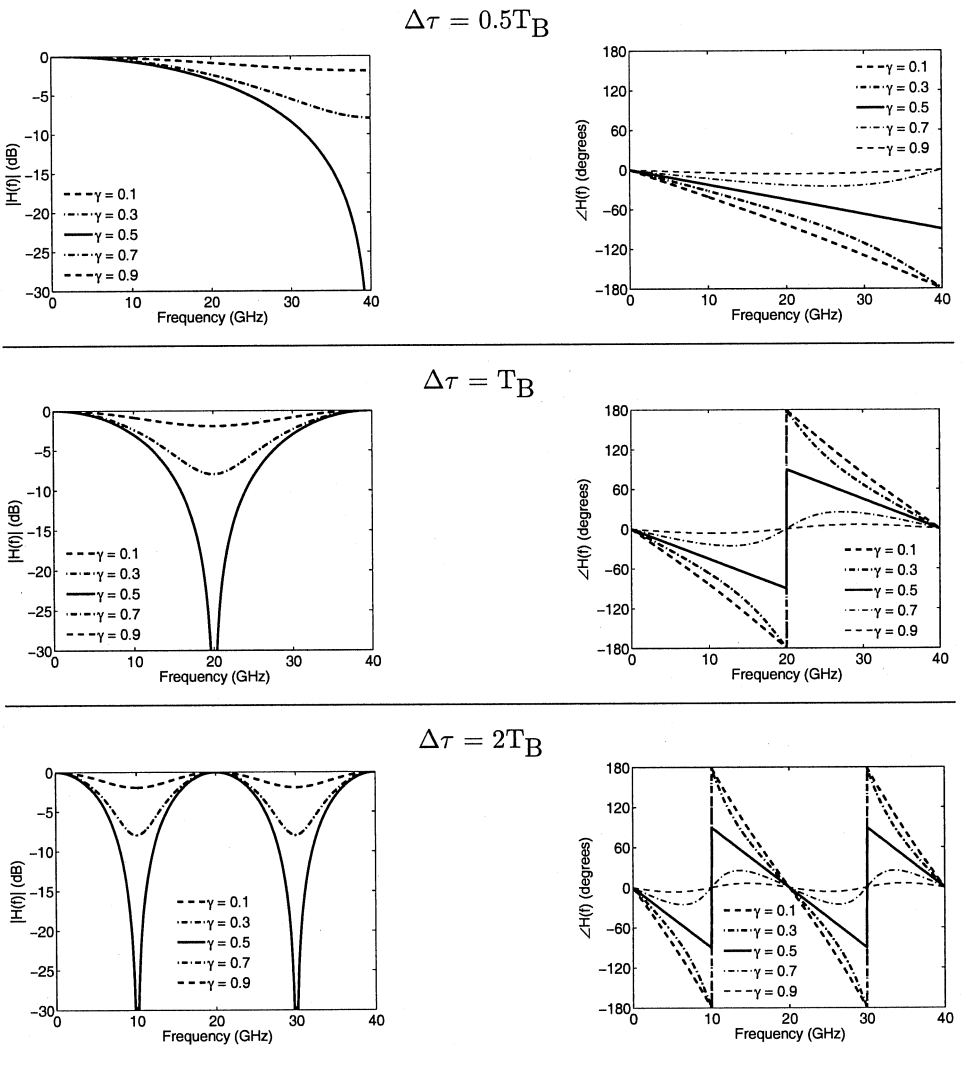

Fig. 3. Magnitude and phase responses of PMD channels with varying γ and $\Delta\tau$ characteristics. T_B is a bit period (e.g. $T_B = \frac{1}{40Gb/s} = 25$ ps at 40 Gb/s).

responses and the possibility of nulls in the frequency spectrum make equalization of this channel difficult.

3. PMD Compensation Methods

Forward error correction (FEC)[20,21] and wavelength redundancy in WDM networks[22] have been suggested as means of mitigating the effects of PMD. However, direct compensation of PMD effects is often required either independent of or in conjunction with redundancy schemes[23,24]. PMD can be directly compensated in

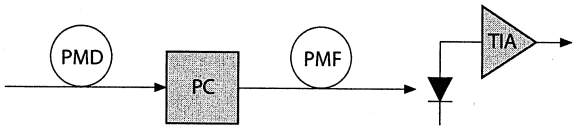

Fig. 4. Simple optical PMD compensator architecture.

any of the optical, optoelectronic and electronic domains. In this section, methods for compensation in each of these domains are described and compared.

3.1. *Optical PMD Compensation*

Optical PMD compensation has been demonstrated to 160 Gb/s[25]. One of the most common optical PMD compensators requires a polarization controller (PC) and a length of polarization-maintaining fiber (PMF), as shown in Figure 4[26]. The PC is used to align the polarization of the light signal such that it is aligned with the the principal states of polarization (PSPs) of the PMF. PMF is fiber which has been intentionally manufactured to have a large, but controlled, birefringence, and therefore can be used to generate a specific amount of DGD. In this way, the power in the fast SOP can be delayed by an amount equal to the DGD of the PMF, resulting in a reduction in the overall DGD. More complicated compensators can be made by replacing the fixed length of PMF with a variable delay to enable cancellation of arbitrary amounts of DGD, or by using multiple PC-PMF stages to increase the degrees of freedom and hence the accuracy of the compensation[12].

Despite the obvious advantages of compensating an optical phenomenon with optical components, optical compensation has several disadvantages. First, optical schemes require expensive and relatively bulky optical components. Also, because of the dynamic nature of PMD, compensators must be adaptive. Adaptation is not easily achieved in the optical domain because of the relative lack of flexibility in optical components, and because of the difficulty in extracting an appropriate error signal to control the adaptation.

3.2. *Optoelectronic PMD Compensation*

It is also possible to compensate PMD using a scheme which involves both the optical and electronic domains. Typically, this scheme involves splitting the received light signal into its two polarization modes by a PC and a polarization beam splitter (PBS)[4]. The resulting light signals are then converted to electrical signals by two separate photodiode-transimpedance amplifier (TIA) front-ends. The electrical signal corresponding to the light in the fast SOP is then delayed by an interval equal to the DGD. Finally, the two signals are recombined to form a received signal that is free from PMD effects. This concept is illustrated in Figure 5.

The main advantage of optoelectronic compensation is that some of the compensation hardware is moved from the optical to the electronic domain, increasing the

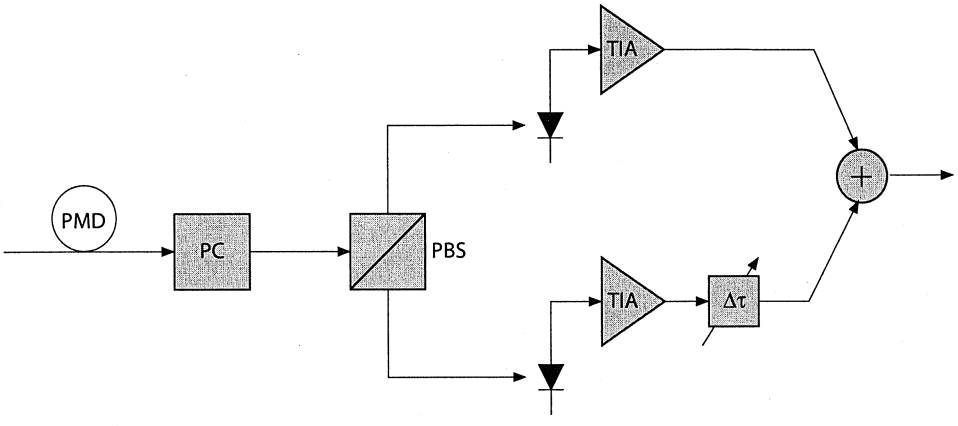

Fig. 5. Typical optoelectronic PMD compensator architecture.

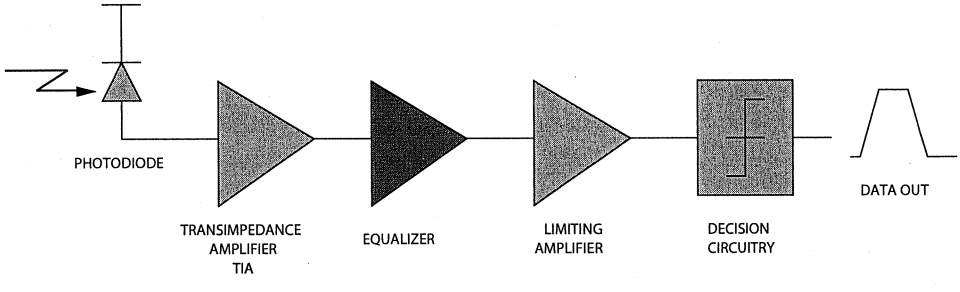

Fig. 6. Block diagram of optical receiver including electronic PMD compensator.

level of integration. However, optoelectronic compensation still requires extra optical components (PC and PBS), so greater integration is possible using an electronic scheme. Also, the addition of a second front-end is a significant expense.

3.3. *Electronic PMD Compensation*

Electronic PMD compensation is performed by equalization of the received signal after it has been converted from light to electricity by a photodiode and TIA. A system diagram of an optical receiver with an equalizer is given in Figure 6.

Electronic equalization is attractive because it offers a higher level of integration and hence a lower cost when compared to optical and optoelectronic solutions. A high level of integration is especially important in WDM systems, in which PMD compensation is required for each channel[4]. Also, the adaptation that is required to track changing PMD conditions is relatively simple to implement electronically, with established adaptation algorithms such as the least mean square (LMS) algorithm readily available. As a result of these considerations, electronic compensation is favoured when it is possible within the bounds of IC technology.

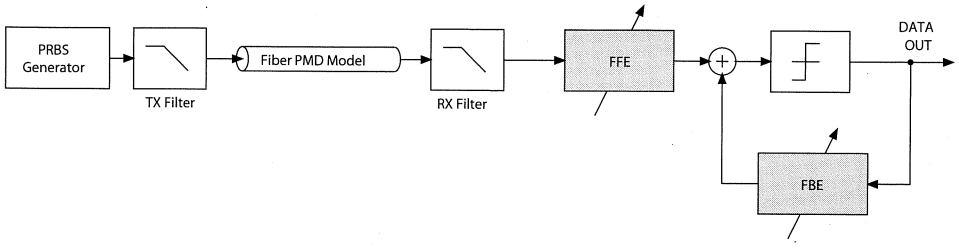

Fig. 7. System model used for Matlab/Simulink simulations.

4. System Model

Matlab/Simulink was used to simulate the effects of PMD in an optical system and to compare various equalizer architectures in terms of their compensation abilities. A simplified block diagram of the system used in these simulations is given in Figure 7. A pseudorandom bit sequence (PRBS) generator is used to generate input data at a rate (R) of 40 Gb/s. This data is passed through a first-order lowpass filter ($f_{3dB} = 0.7 \times R$) used to simulate the effects of the finite bandwidth of the transmitter (TX). It is then passed through an optical fiber model which corrupts the data with PMD. The fiber is modelled using (1). At the output of the fiber model the data is filtered with another first-order lowpass filter ($f_{3dB} = 0.7 \times R$) to simulate the finite bandwidth of the receiver (RX). Equalization is then performed and the equalized waveform is sliced to generate the output data.

Not shown in Figure 7 are the clock recovery and adaptation components of the system. The sampling phase was determined by automatically selecting the clock phase corresponding to the largest eye opening at the output of the channel. Coefficient adaptation for both the FFE and FBE was performed using the LMS algorithm.

Figure 7 shows the equalizer as a DFE, though several equalizer architectures were considered.

5. Equalizer Architectures

5.1. *Analog Equalizer*

Analog or "peaking" equalizers have been used in the past for equalizing simple lowpass channels[27]. The potential advantage of this architecture is its relatively simple implementation. However, the analog equalizer is unsuitable as a PMD compensator because it is not flexible enough to adapt to the wide range of potential PMD conditions. Also, because it is a linear circuit it is unable to compensate for the deep null in the frequency spectrum caused by PMD with γ values near 0.5.

5.2. *IIR Equalizer*

The infinite impulse response (IIR) equalizer would seem to have great potential as a PMD compensator. Because the frequency response of the PMD channel is given by (6), the inverse of the channel transfer function is:

$$H_{\mathrm{PMD}}^{-1}(f) = \frac{1}{\gamma + (1-\gamma)e^{-j2\pi f \Delta\tau}} \tag{8}$$

$H_{\mathrm{PMD}}^{-1}(f)$ also relates the input $X(f)$ and output $Y(f)$ of the inverse filter:

$$H_{\mathrm{PMD}}^{-1}(f) = \frac{Y(f)}{X(f)} \tag{9}$$

Solving for $Y(f)$ we get the input-output relationship:

$$Y(f) = \frac{1}{\gamma}X(f) + \frac{\gamma - 1}{\gamma}e^{-j2\pi f \Delta\tau}Y(f) \tag{10}$$

Taking the inverse Fourier transform of (10) yields a difference equation:

$$y(t) = \frac{1}{\gamma}x(t) + \frac{\gamma - 1}{\gamma}y(t - \Delta\tau) \tag{11}$$

This difference equation describes an IIR filter. While this architecture would seem to offer perfect (zero-forcing) equalization of a PMD channel, the nature of the feedback loop creates problems in practice. Specifically, for $\gamma \leq 0.5$, the equalizer loop gain, which is equal to $\frac{\gamma-1}{\gamma}$ by inspection of (11) is less than -1, meaning that the equalizer is unstable. Thus, since it is unable to compensate PMD for all values of γ, the IIR filter is unsuitable for implementation as a PMD compensator.

5.3. *FIR Equalizer*

The finite impulse response (FIR) filter is a versatile equalizer architecture which is widely used. FIR filters can, given enough taps, approximate any linear transfer function, making them attractive because of their flexibility. However, the usefulness of an FIR filter as a PMD compensator is severely limited because, as a linear filter, it is unable to compensate for the deep nulls caused by PMD with γ values near 0.5.

5.4. *Decision Feedback Equalizer*

Figure 7 illustrates the basic DFE topology. The DFE consists of an FFE and an FBE, both of which can be implemented as FIR filters for maximum flexibility. The most important advantage of the DFE architecture in terms of PMD compensation is that the use of an FBE introduces nonlinear equalization, allowing compensation of the nulls resulting from γ values near 0.5[11]. Because of this, the DFE is the only architecture surveyed that meets the requirements for an electronic PMD compensator.

The main disadvantage of the DFE is its difficult implementation at high speeds, as a result of the feedback loop inherent to the FBE. However, architectural techniques such as the look-ahead DFE architecture[28,29] can alleviate this problem.

6. Simulation Methodology

Having identified the DFE architecture as the most suitable, simulations were performed to identify the performance tradeoffs with respect to the number of equalizer taps in the FFE and FBE. All simulations were performed with symbol-spaced equalizer taps unless otherwise noted.

For each equalizer configuration, it was necessary to consider a wide range of PMD conditions. The DGD, $\Delta\tau$, was varied from 0 to 100 ps (4 bit periods at 40 Gb/s) and γ was varied from 0 to 1. For each ($\Delta\tau$,γ) pair the equalizer was allowed to converge to the ideal tap weights as determined by the LMS algorithm. Then, the ISI penalty was determined by calculating the amount of eye closure using[30]:

$$\text{ISI penalty (dB)} = 10 \times \log_{10}\left(\frac{max.\ eye\ opening}{min.\ eye\ opening}\right) \tag{12}$$

Figure 8 shows representative eye diagrams for the unequalized and equalized case for one particular ($\Delta\tau$,γ) pair. Figure 9 shows surface plots of the ISI penalty with and without an equalizer for one architecture over a wide range of ($\Delta\tau$,γ) pairs. This plot demonstrates the elimination of the penalty pole at $\Delta\tau = 25$ ps, $\gamma = 0.5$ by equalization with a DFE.

Once the ISI penalty had been calculated for all ($\Delta\tau$,γ) pairs, the cumulative probability (CP) of a system outage given a particular power margin was calculated using[15]:

$$\text{CP} = \sum_{(\Delta\tau,\gamma)'} \rho_1(\Delta\tau)\rho_2(\gamma) \tag{13}$$

where $\rho_1(\Delta\tau)$ is the probability distribution of $\Delta\tau$ as described by (2), $\rho_2(\gamma)$ is the probability distribution of γ (uniform)[15] and $(\Delta\tau, \gamma)'$ is the set of $(\Delta\tau, \gamma)$ pairs for which the ISI penalty is greater than the power margin. Power margin represents the ratio of the transmitted power to the transmitted power required for a given BER (e.g. 10^{-12}). When the ISI penalty exceeds the power margin, a system outage occurs because the excess transmitted power cannot overcome the eye closure caused by the ISI, and the BER increases above the specified maximum tolerable level.

As described in Section 2.1, $\rho_1(\Delta\tau)$ depends on the average DGD of the particular fiber. For each equalizer configuration, the probability distribution was varied by adjusting the average DGD to find the maximum average DGD that would result in a CP of less than 10^{-6} (30 seconds per year).

To summarize, for each equalizer configuration (number of taps) the ISI penalty contour is calculated over all γ and $\Delta\tau$. For a given power margin, the $(\gamma, \Delta\tau)'$ pairs corresponding to a system outage are those pairs that give an ISI penalty greater than the power margin. The joint probabilities of occurrence for all of the $(\gamma, \Delta\tau)'$

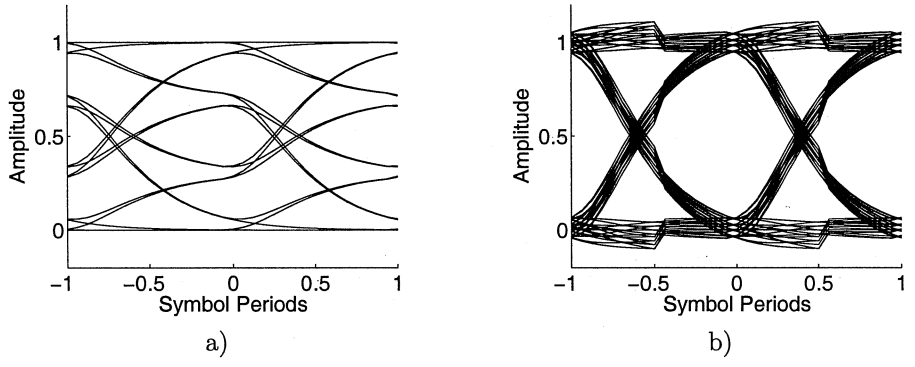

Fig. 8. Eye diagrams for $\Delta\tau = 25$ ps, $\gamma = 0.3$. a) No equalization. b) Equalization by 3-tap FFE and 1-tap FBE.

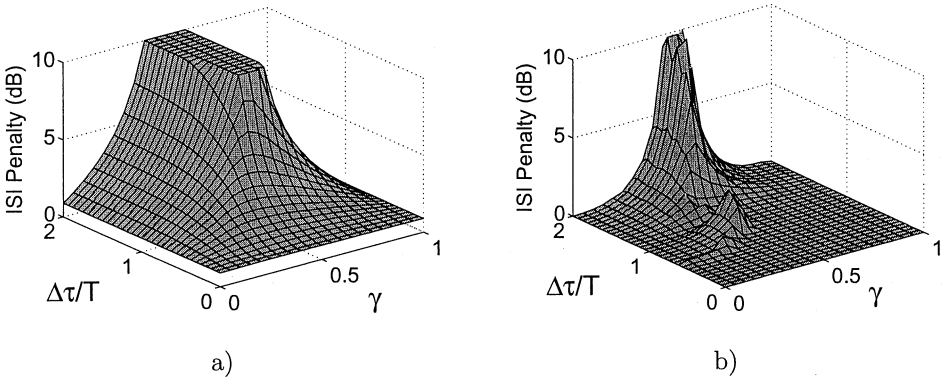

Fig. 9. ISI penalty vs. $\Delta\tau$ and γ. ISI penalty is truncated at 10 dB. a) No equalization. b) Equalization by 3-tap FFE and 1-tap FBE.

pairs contributing to system outage are then summed to find the overall system outage probability. As long as this overall system outage probability remains lower than 10^{-6}, the average DGD is increased and the calculation repeated. The maximum average DGD that results in an overall outage probability of less than 10^{-6} is then recorded as a measure of performance for comparison with other equalizer configurations.

7. Simulation Results

Figures 10, 11 and 12 show the results of these simulations for DFEs with no FBE, a 1-tap FBE and a 2-tap FBE, respectively. In each case, the maximum average DGD that is tolerable from a system point of view is plotted against the power margin for different numbers of FFE taps. In addition, the unequalized case is included as a reference for comparison. Figure 10 shows that using an FFE only, a modest

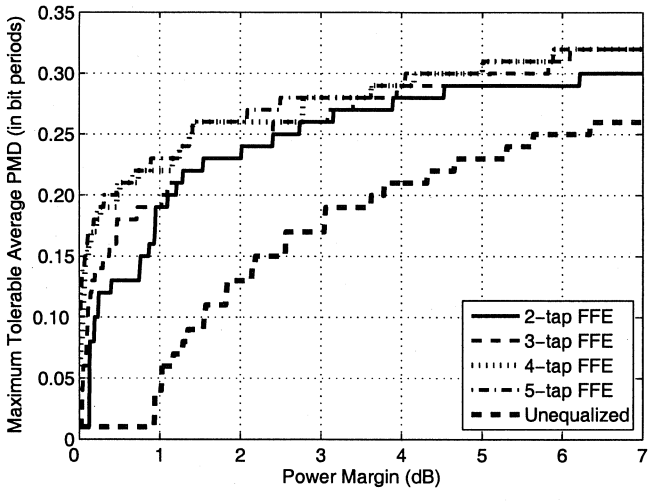

Fig. 10. Plot of maximum tolerable PMD vs. power margin for FFEs with varying number of taps (No FBE).

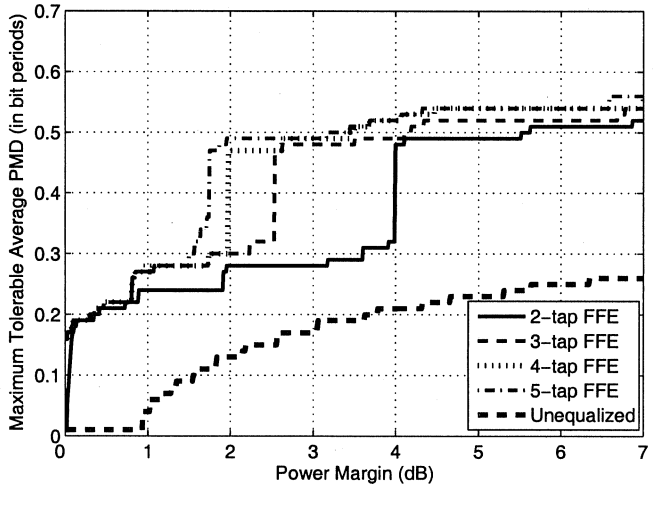

Fig. 11. Plot of maximum tolerable PMD vs. power margin for FFEs with varying number of taps (1-tap FBE).

increase in maximum average DGD is possible, from roughly $0.15T_b$ to $0.25T_b$ at a power margin of 2-3 dB. Only minor improvements are achievable by increasing the number of FFE taps because regardless of the number of taps the FFE is unable to compensate for the case $\Delta\tau = 25$ ps, $\gamma = 0.5$. Figure 11 demonstrates that by using a 1-tap FBE, a significant performance increase is possible, with the maximum

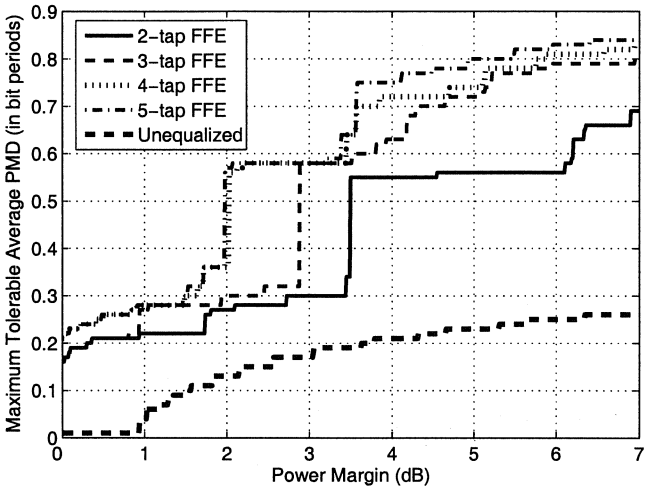

Fig. 12. Plot of maximum tolerable PMD vs. power margin for FFEs with varying number of taps (2-tap FBE).

average DGD increasing to approximately $0.5T_b$. For this case, the number of FFE taps offering the best balance between performance and complexity is dependent on the power margin. For power margins below 3 dB, four taps offer the best balance, while three taps offer the best balance for power margins above 3 dB. Figure 12 shows that a further increase in maximum average DGD is possible by using a 2-tap FBE, but significant gains are limited to power margins above 4 dB. Once again, four FFE taps offer the best balance for power margins below 3 dB, while three taps offer the best balance for power margins above 3 dB.

Figure 13 shows the maximum average DGD plotted against the number of FFE taps for a power margin of 3 dB. Once again, the unequalized case is included for comparison. This plot more clearly shows the performance of each of the equalizer architectures. It is clear from this plot that for a power margin of 3 dB, a 3-tap FFE offers performance nearly equal to the more complex 4- and 5-tap FFEs. As expected, the 2-tap FBE offers a modest performance increase over the 1-tap FBE. However, the 1-tap FBE may be a more attractive choice when this performance increase is weighed against the added complexity of a second tap. This is particularly true if a look-ahead architecture is employed for the FBE (as is likely the case) since the FBE complexity would increase exponentially with the number of taps.

These results are significant because they imply that the useful length of high-speed optical systems affected by PMD can be greatly increased by including electronic PMD compensation in the form of a DFE with modest complexity. To keep system outage levels at an acceptable level, $\Delta\tau_{avg}$ must be less than the maximum average DGD. Therefore, using (4) it is found that the useful length of the fiber increases with the square of the increase in maximum average DGD. As an exam-

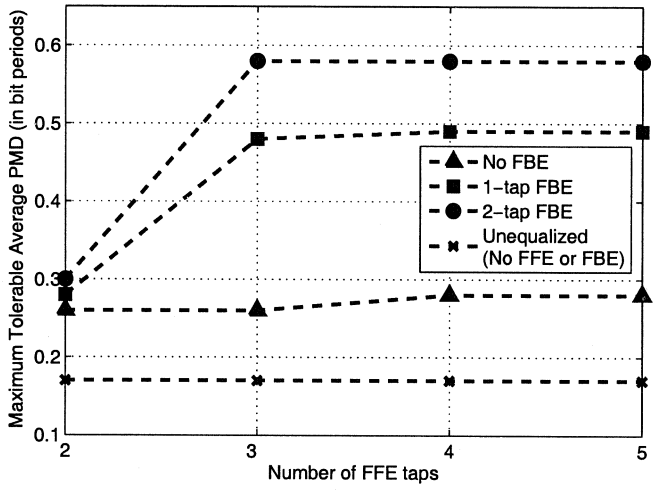

Fig. 13. Plot of maximum tolerable PMD vs. number of FFE taps for no FBE, 1-tap FBE and 2-tap FBE at a power margin of 3 dB.

ple, consider a 40-Gb/s system for which the PMD of the fiber is 1.0 ps/$\sqrt{\text{km}}$, and the power margin is 3 dB. From Figure 13, the maximum average DGD for an unequalized system at a power margin of 3 dB is $0.17T_b$, corresponding to a maximum fiber length of 18 km, using (4). The maximum average DGD for a system using a DFE with a 3-tap FFE and 1-tap FBE is $0.49T_b$, corresponding to a maximum fiber length of 150 km. Hence, an increase in maximum length of more than eight times is achieved by equalization. At these lengths, other impairments (such as noise and CD) would likely replace PMD as reach-limiting factors. Therefore, the combination of a 3-tap FFE and 1-tap FBE is all that is required to effectively eliminate PMD as the dominant length-limiting factor in most 40-Gb/s optical systems.

7.1. *Fractionally-Spaced Equalization*

Fractionally-spaced equalizers (FSEs), for which the tap spacing is $T_B/2$, were also considered for the FFE. Figure 14 shows the maximum average PMD for fractionally-spaced and symbol-spaced FFEs with a 1-tap FBE for a system power margin of 3 dB. The two equalizer configurations are compared in terms of equalizer span, i.e. the difference in delay between the first tap and the last tap of the equalizer. Equalizer span is important in PMD compensation because it determines the maximum amount of DGD that the equalizer can handle. Furtermore, when distributed circuit techniques are employed for implementation of the FFE, equalizer complexity is generally proportional to the span, not the number of taps. From this plot, it is seen that for a given span, the FSE provides a performance increase over the symbol-spaced equalizer. However, the gain through each tap of an FSE

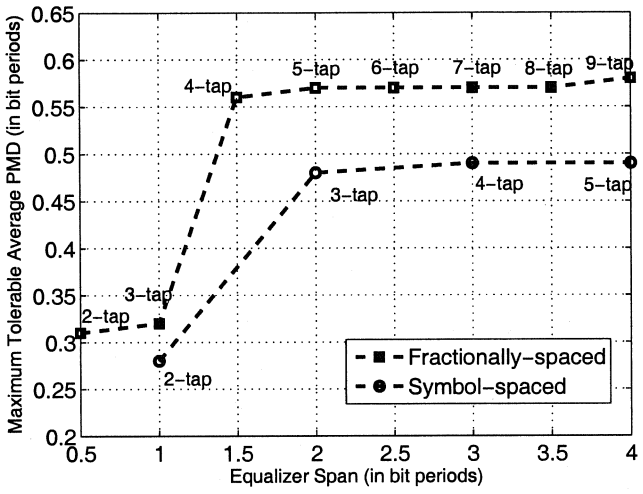

Fig. 14. Plot of maximum tolerable PMD vs. equalizer span for fractionally-spaced and symbol-spaced FFEs and a 1-tap FBE at a power margin of 3 dB.

based upon distributed circuit techniques will be limited to one half that through each tap of a symbol-spaced equalizer because of topological considerations. For cases where noise is the limiting factor and only one equalizer tap is needed (e.g. a long fiber that happens to have negligible PMD), an FSE with only half the tap gain will require a power margin 3 dB higher than a symbol-spaced equalizer for equal performance. Therefore, the performance increase demonstrated in Figure 14 is exaggerated somewhat. Also, increasing the number of taps by decreasing the tap spacing increases the complexity of the adaptation required, making it more difficult to achieve convergence of tap values. For these reasons, a symbol-spaced equalizer is often preferred.

7.2. *Variable Tap Delays*

One observation from these simulations is that the usefulness of a PMD compensator is limited by its span. An equalizer is powerless to compensate for PMD with DGD exceeding its span. To increase the amount of DGD that can be compensated, more taps can be added. However, in a PMD compensator with many taps, only the first taps will be utilized for small DGD values while only the first and last taps will be utilized for large DGD values. Alternatively, an equalizer with only a few taps can perform comparably to one with many taps if the tap delays can be made variable. Variable tap delays allow the tap spacing to be aligned with the DGD, maximizing the compensation accuracy with the fewest possible taps. However, there is currently no acceptable method of implementing variable delays on integrated circuits with the required tuning range and bandwidth.

8. Conclusions

A system-level analysis using Matlab/Simulink has been used to compare the performance of different electronic PMD compensator architectures at 40 Gb/s. It has been demonstrated that equalization by a DFE with a 3-tap FFE and a 1-tap FBE is able to increase by nearly three times the maximum average DGD that is tolerable from a system point of view, from $0.17T_b$ to $0.49T_b$. This is significant because it effectively eliminates PMD as the dominant length-limiting factor in most 40-Gb/s optical systems. In addition to the many practical considerations favoring electronic compensation over optical and optoelectronic methods, the complexity of the required equalizer is modest, with prototype integrated circuits meeting these requirements having already been reported[9].

Acknowledgments

This work has been supported by grants from the Natural Sciences and Engineering Research Council of Canada (NSERC), Gennum Corporation and Micronet.

References

1. J. Hecht, *City of Light: The Story of Fiber Optics.* New York: Oxford University Press, 1999.
2. K. Azadet, E. F. Haratsch, H. Kim, F. Saibi, J. H. Saunders, M. Shaffer, L. Song, and M. L. Yu, "Equalization and FEC techniques for optical transceivers," *IEEE Journal of Solid-State Circuits*, vol. 37, no. 3, pp. 317–327, Mar. 2002.
3. H. Bülow, "Polarisation mode dispersion (PMD) sensitivity of a 10 Gbit/s transmission system," in *Optical Communication, 1996. ECOC '96. 22nd European Conference on*, vol. 2, 1996, pp. 211–214.
4. ——, "PMD mitigation techniques and their effectiveness in installed fiber," in *Optical Fiber Communication Conference, 2000*, vol. 3, 2000, pp. 110–112.
5. H. Bülow, W. Baumert, H. Schmuck, F. Mohr, T. Schulz, F. Kuppers, and W. Weiershausen, "Measurement of the maximum speed of PMD fluctuation in installed field fiber," in *Optical Fiber Communication Conference, 1999, and the International Conference on Integrated Optics and Optical Fiber Communication. OFC/IOOC '99. Technical Digest*, vol. 2, 1999, pp. 83–85.
6. H. Wu, J. A. Tierno, P. Pepeljugoski, J. Schaub, S. Gowda, J. A. Kash, and A. Hajimiri, "Integrated transversal equalizers in high-speed fiber-optic systems," *IEEE Journal of Solid-State Circuits*, vol. 38, no. 12, pp. 2131–2137, Dec. 2003.
7. H. Bülow, F. Buchali, W. Baumert, R. Ballentin, and T. Wehren, "PMD mitigation at 10 Gbit/s using linear and nonlinear integrated electronic equaliser circuits," *Electronics Letters*, vol. 36, no. 2, pp. 163–164, 2000.
8. L. Möller, S. Thiede, S. Chandrasekhar, W. Benz, M. Lang, T. Jakobus, and M. Schlechtweg, "ISI mitigation using decision feedback loop demonstrated with PMD distorted 10Gbit/s signals," *Electronic Letters*, vol. 35, no. 24, pp. 2092–2093, 1999.
9. M. Nakamura, H. Nosaka, M. Ida, K. Kurishima, and M. Tokumitsu, "Electrical PMD equalizer ICs for a 40-Gbit/s transmission," in *Optical Fiber Communication Conference and Exhibit, 2004. OFC 2004*, vol. TuG4, 2004.
10. A. Hazneci and S. P. Voinigescu, "A 49-Gb/s, 7-tap transversal filter in 0.18μm SiGe

BiCMOS for backplane equalization," in *IEEE Compound Semiconductor Integrated Circuits Symposium*, Monterey, CA, Oct. 2004.
11. H. Bülow and G. Thielecke, "Electronic PMD mitigation - from linear equalization to maximum-likelihood detection," in *Optical Fiber Communication Conference and Exhibit, 2001. OFC 2001*, vol. 3, 2001, pp. WAA3–1–WAA3–3.
12. H. Sunnerud, C. J. Xie, M. Karlsson, R. Samuelsson, and P. A. Andrekson, "A comparison between different PMD compensation techniques," *IEEE/OSA Journal of Lightwave Technology*, vol. 20, no. 3, pp. 368–378, Mar. 2002.
13. B. Razavi, *Design of Integrated Circuits for Optical Communications.* New York: McGraw-Hill, 2003.
14. C. D. Poole, R. W. Tkach, A. R. Chraplyvy, and D. A. Fishman, "Fading in lightwave systems due to polarization-mode dispersion," *IEEE Photonics Technology Letters*, vol. 3, no. 1, pp. 68–70, Jan. 1991.
15. H. Bülow, "Operation of digital optical transmission system with minimal degradation due to polarisation mode dispersion," *Electronic Letters*, vol. 31, no. 3, pp. 214–215, 1995.
16. G. J. Foschini and C. D. Poole, "Statistical-theory of polarization dispersion in single-mode fibers," *IEEE/OSA Journal of Lightwave Technology*, vol. 9, no. 11, pp. 1439–1456, Nov. 1991.
17. N. Gisin, R. Passy, J. C. Bishoff, and B. Perny, "Experimental investigations of the statistical properties of polarization mode dispersion in single mode fibers," *IEEE Photonics Technology Letters*, vol. 5, no. 7, pp. 819–821, July 1993.
18. R. Ramaswami and K. N. Sivarajan, *Optical Networks - A Practical Perspective, Second Edition.* Morgan Kaufmann Publishers, 2002.
19. F. Buchali and H. Bülow, "Adaptive PMD compensation by electrical and optical techniques," *IEEE/OSA Journal of Lightwave Technology*, vol. 22, no. 4, pp. 1116–1126, Apr. 2004.
20. B. Wedding and C. N. Haslach, "Enhanced PMD mitigation by polarization scrambling and forward error correction," in *Optical Fiber Communication Conference and Exhibit, 2001. OFC 2001*, vol. 3, 2001, pp. WAA1–1–WAA1–3.
21. L. Song, M.-L. Yu, and M. S. Shaffer, "10- and 40-Gb/s forward error correction devices for optical communications," *IEEE Journal of Solid-State Circuits*, vol. 37, no. 11, pp. 1565–1573, Nov. 2002.
22. D. Penninckx, S. Lanne, and H. Bülow, "WDM redundancy to counteract PMD effects in optical systems," in *Optical Communication, 2001. ECOC '01. 27th European Conference on*, vol. 3, 2001, pp. 444–445.
23. H. F. Haunstein, W. Sauer-Greff, A. Dittrich, K. Sticht, and R. Urbansky, "Principles for electronic equalization of polarization-mode dispersion," *IEEE/OSA Journal of Lightwave Technology*, vol. 22, no. 4, pp. 1169–1182, Apr. 2004.
24. H. Sunnerud, M. Karlsson, C. J. Xie, and P. A. Andrekson, "Polarization-mode dispersion in high-speed fiber-optic transmission systems," *IEEE/OSA Journal of Lightwave Technology*, vol. 20, no. 12, pp. 2204–2219, Dec. 2002.
25. H. Sunnerud, M. Westlund, J. Li, J. Hansryd, M. Karlsson, P.-O. Hedekvist, and P. A. Andrekson, "Long-term 160 Gb/s-TDM, RZ transmission with automatic PMD compensation and system monitoring using an optical sampling system," in *Optical Communication, 2001. ECOC '01. 27th European Conference on*, vol. 6, 2001, pp. 18–19.
26. C. Francia, J.-P. Bruyère, F. Thiéry, and D. Penninckx, "Simple dynamic polarisation mode dispersion compensator," *Electronics Letters*, vol. 35, no. 5, pp. 414–415, 1999.
27. G. Zhang, P. Chaudhari, and M. Green, "26.7 - a BiCMOS 10Gb/s adaptive ca-

ble equalizer," in *Solid-State Circuits Conference, 2004. Digest of Technical Papers. ISSCC. 2004 IEEE International*, 2004, pp. 482–491.

28. S. Kasturia and J. H. Winters, "Techniques for high-speed implementation of nonlinear cancellation," *IEEE J. Selected Areas in Communications*, vol. 9, no. 5, pp. 711–717, June 1991.
29. Y.-S. Sohn, "A 2.2 gbps CMOS look-ahead dfe receiver for multidrop channel with pin-to-pin time skew compensation," in *IEEE Custom Integrated Circuits Conference*, Sept. 2003, pp. 473–476.
30. P. Pepeljugoski, S. E. Golowich, A. J. Ritger, P. Kolesar, and A. Risteski, "Modeling and simulation of next-generation multimode fiber links," *IEEE/OSA Journal of Lightwave Technology*, vol. 21, no. 5, pp. 1242–1255, May 2003.